

Aldehyde dehydrogenase activity promotes survival of human muscle precursor cells

Elise Jean^{a, b}, Dalila Laoudj-Chenivesse^{a, b}, Cécile Notarnicola^{a, b}, Karl Rouger^c, Nicolas Serratrice^d, Anne Bonniou^e, Stéphanie Gay^e, Francis Bacou^e, Cédric Duret^{f, g}, and Gilles Carnac^{a, b, *}

^a INSERM, ERI 25, Muscle et Pathologies, Montpellier, France

^b Université Montpellier I, Montpellier, France

^c INRA, UMR703, Développement et Pathologie du Tissu Musculaire, Ecole Nationale Vétérinaire, Nantes, France

^d IGMM CNRS 5535 – Université Montpellier I et II, Montpellier, France

^e INRA, UMR866, Différenciation Cellulaire et Croissance, Montpellier, France.

^f INSERM, U632, Montpellier, France

^g Université Montpellier 1, UMR-S632, Montpellier, France

Received: June 15, 2009; Accepted: October 5, 2009

Abstract

Aldehyde dehydrogenases (ALDH) are a family of enzymes that efficiently detoxify aldehydic products generated by reactive oxygen species and might therefore participate in cell survival. Because ALDH activity has been used to identify normal and malignant cells with stem cell properties, we asked whether human myogenic precursor cells (myoblasts) could be identified and isolated based on their levels of ALDH activity. Human muscle explant-derived cells were incubated with ALDEFLUOR, a fluorescent substrate for ALDH, and we determined by flow cytometry the level of enzyme activity. We found that ALDH activity positively correlated with the myoblast-CD56⁺ fraction in those cells, but, we also observed heterogeneity of ALDH activity levels within CD56-purified myoblasts. Using lentiviral mediated expression of shRNA we demonstrated that ALDH activity was associated with expression of Aldh1a1 protein. Surprisingly, ALDH activity and Aldh1a1 expression levels were very low in mouse, rat, rabbit and non-human primate myoblasts. Using different approaches, from pharmacological inhibition of ALDH activity by diethylaminobenzaldehyde, an inhibitor of class I ALDH, to cell fractionation by flow cytometry using the ALDEFLUOR assay, we characterized human myoblasts expressing low or high levels of ALDH. We correlated high ALDH activity *ex vivo* to resistance to hydrogen peroxide (H₂O₂)-induced cytotoxic effect and *in vivo* to improved cell viability when human myoblasts were transplanted into host muscle of immune deficient *scid* mice. Therefore detection of ALDH activity, as a purification strategy, could allow non-toxic and efficient isolation of a fraction of human myoblasts resistant to cytotoxic damage.

Keywords: ALDH • satellite cells • myoblast • adult stem cells • skeletal muscle

Introduction

Skeletal muscle has the ability to undergo rapid repair after acute damage. This process is driven by a group of highly specialized cells – known as ‘satellite cells’ – that are found beneath the basal lamina surrounding each myofibre. While normally quiescent, satellite cells become activated upon muscle damage and start to proliferate. Then, their descendants, the myoblasts, differentiate and fuse to regenerate the damaged muscle. Beside these criteria,

satellite cells can be identified by the expression of specific combinations of molecular markers, the most widely used in mouse are probably Pax7, M-cadherin and CD34 [1]. Because myoblasts can be transplanted and fuse with endogenous muscle fibres to form hybrid myotubes [2], myoblast transplantation represents a potential approach for the treatment of inherited myopathies and diseases characterized by fibre necrosis and muscle weakness [3–6]. Although other limitations, such as immune rejection or limited spread into the host tissue are also important, failure of myoblast transfer in the initial clinical trials was at least partly related to poor survival rate of transplanted myoblasts [3, 5–7]. Several approaches have been developed to reduce early loss of injected myoblasts: immunosuppressive treatment to reduce inflammation [8, 9], heat shock treatment of grafted myoblasts to

*Correspondence to: Gilles CARNAC,
INSERM, ERI 25, Muscle et Pathologies,
F-34295 Montpellier, France.
Tel.: +33 (0) 4 67 41 52 25
Fax: +33 (0) 4 67 41 52 31
E-mail: gilles.carnac@inserm.fr

improve their resistance to apoptosis [10], control of growth factor levels to increase myoblast proliferation [11, 12] and neo-angiogenesis to reduce hypoxia and cell death [13]. One additional approach would be to select and purify a pool of myoblasts characterized by an improved survival response. Recent studies reached high efficiency of mouse myoblast transplantation after using cell-surface markers to purify a myoblast subpopulation [14]. Thus, manipulating myoblast subpopulations may have important implications for development of new treatments. However, to date, only a small number of surface markers are available to isolate human myoblasts, the most widely used being CD56 Suppress (N-CAM) [15, 16]. Thus, it is important to characterize other markers of human muscle progenitors in order to identify and manipulate them efficiently.

Aldehyde dehydrogenases (ALDH) are a family of enzymes that efficiently oxidize and detoxify aldehydic products of lipid peroxidation such as 4-hydroxynonenal, which are initially generated by reactive oxygen species [17, 18]. In addition to its protective role against toxic molecules, a subfamily of ALDH is involved in retinoic acid synthesis. These retinaldehyde dehydrogenases belong to the ALDH 1, 2 and 3 subfamilies [17]. Retinoic acid binds and activates nuclear retinoic acid receptor/retinoic X receptor heterodimers to regulate the transcription of target genes important for stem cell differentiation [19]. Compelling evidence suggests that ALDH activity is associated with the stem cell status of cells in haematopoietic and nerve tissues. Indeed, selection based on high ALDH activity allows the isolation of long-term reconstituting human haematopoietic stem cells [20, 21]. This observation has been extended to other transplantable cells. Corti *et al.* showed that high activity of ALDH characterizes a primitive brain-derived neural stem cell population [22]. Recently, ALDH has been identified as a marker of normal and malignant human mammary stem cells [23, 24]. Therefore, it appears that ALDH confers a specific advantage to stem cells, but the molecular nature of this advantage is not clear. In summary, ALDH could enhance cell survival, stem cell renewal, proliferation or differentiation.

Here, we assessed human myogenic precursor cells (myoblasts) for ALDH functional activity. We used fluorescence-activated cell sorting (FACS) coupled to ALDEFLUOR – a fluorescent substrate for ALDH – and *ex vivo* and *in vivo* functional assays to characterize differences between human myoblast populations expressing low or high levels of ALDH. Our findings suggest that high ALDH activity is restricted to a fraction of human myoblasts and is associated with improved cell viability.

Materials and methods

Primary human muscle cell culture

Quadriceps muscle biopsies of nine human adults (mean age 34 years \pm 3.02) were obtained from the 'AFM-BTR Banque de tissus pour la recherche' (Hôpital de la PitiéSalpêtrière, Paris, France) and from patients

followed at the Service de Physiologie Clinique, Centre Hospitalier Universitaire Lapeyronie (Montpellier, France). Informed and written consent was obtained from all persons after explanation of the protocol. Skeletal muscle explant-derived cells were initially prepared. Muscle biopsies (50 mg) were scissor minced and tissue fragments were plated in collagen-coated dishes. Explants were anchored to the dish by a thin layer of Matrigel® (BD Biosciences, Le Pont De Claix, France) and maintained in growth medium composed of DMEM (Sigma-Aldrich, Saint Quentin Fallavier, France), 20% foetal calf serum (FCS) (Thermo Fisher Scientific, Illkirch, France) and 0.5% Ultrosor G (Pall, France) at 37°C in 95% humidified air, with 5% CO₂. After 6 to 8 days, cells migrated out of the explants. Migrating cells were enzymatically harvested using dispase (BD Biosciences) and subcultured in growth medium. On average, 30% of the total cells expressed desmin, a marker of myogenic cells (unpublished observations). To purify myoblasts, an immunomagnetic sorting system with magnetic activated cell sorter (MACS) microbeads (Miltenyi Biotec, Paris, France) directly linked to an antibody against N-CAM (CD56) was used [15]. CD56⁺ cells were isolated and enriched according to the manufacturer's instructions and were at least 99% positive for desmin expression. When CD56-purified human myoblasts reached confluency, differentiation was induced by serum depletion (2% FCS). Cells were kept in differentiation medium for 2–4 days. Note that in the manuscript, 'human myoblasts' (hm) is commonly used instead of 'CD56-purified' human myoblasts. There is one exception reported in Table 1 where human myoblasts were prepared by 'pronase digestion' according to the protocol set up for mice, rat and rabbit satellite cells.

To determine whether ALDH activity reflects *Aldh1a1* expression in human myoblasts, we used lentiviral mediated expression of *Aldh1a1* shRNA (MISSION shRNA Control Transduction Particles, Sigma-Aldrich). Human myoblasts were infected on day 0 as indicated by the manufacturer. On day 2, we added 0.5 μ g of puromycin in culture medium for selection of transduced cells. On day 6, fresh medium was added. Then, Western blot and flow cytometry analysis were performed. shRNA lentiviral constructs TRCN0000026498 (shAldh1a1–98) and TRCN0000026482 (shAldh1a1–82), the most efficient in inhibiting *Aldh1a1*, target 5'sequences of *Aldh1a1* mRNA.

Primary mouse, rat, rabbit muscle cell cultures

Briefly, satellite cells were isolated from the whole mice muscles of the paw and from rat leg muscles after enzymatic digestion by pronase [25, 26]. Rabbit satellite cells were isolated from the semi-membranous accessorius muscle as previously described [26]. Cells were plated at a density of 2×10^4 cells/cm² on Matrigel®-coated Petri dishes (BD Biosciences), in 80% Ham's F10 supplemented with 20% horse serum (Invitrogen, Cergy Pontoise, France). They were maintained at 37°C in a water-saturated atmosphere containing 5% CO₂ in air. After 2 days, cells were washed with Ham's F10 and placed in complete medium supplemented with 5 ng/ml basic fibroblast growth factor. Cells were harvested at day 3.

Primary non-human primate muscle cell cultures

Cells were isolated from the appendicular muscles of 5-years old non-human primates, housed and cared for at the Boisbonne Center for Gene Therapy of the National Veterinary School of Nantes (France). Non-human primates were captive-bred *Macacus cynomolgus* macaques purchased from BioPrim (Baziège, France). The Institutional Animal Care and Use

Committee of the French National Institute for Agronomic Research (INRA) approved the protocol [27, 28]. Muscles were minced with scissors and incubated in 199 medium (M199, VWR, Fontenay Sous Bois, France) with 1% type-VIII collagenase (Sigma-Aldrich) and 0.2% type 1-S hyaluronidase (Sigma-Aldrich) at 37°C for 15 min. The digested material was spun down at $150 \times g$ for 10 min. and the supernatant containing the released cells was collected. Satellite cells were diluted in growth medium (44% DMEM, [VWR], 44% M199, 10% FCS [Sigma-Aldrich]). Cells were seeded at 30,000 cells/cm² in gelatin-coated flasks and routinely grown at 37°C in a 5% CO₂ atmosphere.

Isolation of epithelial and stromal corneal cells for flow cytometry

This protocol was adapted from the dissociation procedure that uses collagenase digestion [29]. C57Bl6 mice were killed: eye balls and corneas were removed in PBS on ice. Corneal endothelium was dissected under a binocular microscope. Corneal epithelium and stroma were digested with fresh collagenase B (1 mg/ml, Roche Applied Science, Meylan, France) at 37°C with shaking for 45 min. After low speed centrifugation ($250 \times g$, 5 min.) pellets were diluted and passed through a cell strainer. Cells were analysed with a FACS Calibur flow cytometer (BD Biosciences). Data analysis was performed with CellQuestPro (BD Biosciences).

Western blot analysis

Cells were lysed in hypotonic buffer (50 mM Tris pH 7.5) and protein concentrations were determined using the BioRad Protein Assay. A total of 20 µg of total proteins diluted in 1× Laemmli buffer (100 mM Tris-HCl, pH 6.8, 4% SDS) were separated by SDS-PAGE gel electrophoresis and transferred to PVDF membranes (Millipore, Molsheim, France), blocked 1 hr at room temperature with 5% milk in PBS and probed at 4°C overnight with the following primary antibodies: polyclonal anti-Aldh1a1 and anti-Aldh1a2 (Santa Cruz Biotechnology, Inc., Heidelberg, Germany) diluted 1/500; monoclonal anti-tubulin α (Sigma-Aldrich) diluted 1/10,000; polyclonal anti-MyoD (Santa Cruz Biotechnology, Inc.) diluted 1/500; monoclonal anti-MHC slow and fast (Sigma-Aldrich) diluted 1/500; monoclonal anti-Pax7 supernatant (Developmental Studies Hybridoma Bank, Iowa City, IA, USA) diluted 1/2; polyclonal anti-Myf5 (Santa Cruz Biotechnology, Inc.) diluted 1/500; monoclonal anti-desmin (Sigma-Aldrich) diluted 1/1000; monoclonal anti-troponin T (Sigma-Aldrich) diluted 1/1000; monoclonal anti-caveolin-3 (BD Biosciences) diluted 1/500. Membranes were washed in PBS and incubated with a horseradish peroxidase-conjugated anti-mouse or anti-goat antibody (GE Healthcare, Orsay, France).

Immunofluorescence

Human myoblasts were fixed in PBS containing 4% paraformaldehyde (Electron Microscopy Sciences, Ayguesvives, France) and permeabilized with PBS 0.5% triton X-100. Monoclonal anti-desmin or monoclonal anti-troponin T (Sigma-Aldrich) and rabbit polyclonal anti-myogenin (Santa Cruz Biotechnology, Inc.) were added at a dilution of 1/200 before secondary incubation with Alexa 488-conjugated anti-mouse antibody (Invitrogen). For CD56 staining, living cells were successively incubated with CD56 antibodies (1/1000) and Alexa 555-conjugated anti-mouse antibody. Cells were then fixed and processed for immunofluorescence.

After implantation, serial frozen sections of quadriceps were prepared and stained with rabbit polyclonal antibodies anti-dystrophin [30] and mouse monoclonal anti-lamin A/C (Novocastra; Leica Microsystems Sas, Nanterre, France). Rabbit polyclonal was revealed with Alexa 555-conjugated anti-rabbit antibody whereas mouse monoclonal was revealed with Alexa 647-conjugated anti-mouse antibody (1/1000). Nuclei were revealed by DAPI staining.

Quantitative RT-PCR

Total RNA was extracted from ALDH^{high} and ALDH^{low} human myoblasts, mice corneal cells and primary mouse myoblasts using standard manufacturer's protocols (High Pure RNA Isolation kit, Roche Diagnostics, Meylan, France). Synthesis of cDNA was carried out using the SuperScript[®] II Reverse Transcriptase (Roche Diagnostics). To quantify *Aldh1a1* expression we used the real-time RT-PCR LightCycler technology (Roche Diagnostics, France; 95°C for 10 sec., 60°C for 5 sec., 72°C for 10 sec.). PCR primers were designed using the LightCycler probe design2 software 5 (Roche Diagnostics) and tested for homology with other sequences at the NCBI gene BLAST website. mRNA values were determined by Lightcycler analysis software (version 3.5, Roche) according to the standard curves. Data were represented as the mean level of *Aldh1a1* expression relative to *28S* standard expression.

Genes	Primers	Accession no.
Human 28s	F-TTCACCCACTAATAGGGAACG	NR_003287.2
	R-CCTCAGCCAAGCACATAC	
Mice 28s	F-ATTGTTCACCCACTAATAGGGA	NR_003279.1
	R-GCCAAGCACATACACAAA	
Human ALDH1A1	F-ATGGATGCTTCGAGAGG	NM_000689.3
	R-GCCACATACACCAATAGGTTT	
Mice ALDH1A1	F-TAGCAGCAGGACTCTTCACTAA	NM_013467
	R-TCACCCAGTTCTTCCATTT	
Human ALDH3A1	F-CCTACTATGAGGAGGTGGTGT	NM_000691
	R-GGCTGGATGGTGGGTTT	
Mice ALDH3A1	F-CAGCCTTCACGATACATAGC	NM_007436
	R-ACACATAGAGTGCCAGGG	

Flow cytometry

Cells obtained from muscle explants as 'explant-derived' or CD56⁺ were suspended in ALDEFUOR assay buffer and incubated for 30 min. according to the manufacturer's specifications (StemCell Technologies, Grenoble, France). In each experiment, an aliquot of cells was incubated under identical conditions with the specific ALDH inhibitor diethylaminobenzaldehyde (DEAB) as negative control. The amount of intracellular fluorescence was measured by flow cytometry using a FACS Calibur (BD Biosciences) and analysed using the CellQuestPro Software (BD Biosciences). ALDH^{high} (top 5% of the parent population) and ALDH^{low} cells (bottom 5% of the parent population) were selected with FACS ARIA (BD Biosciences) (C. Duperray, Montpellier RIO Imaging facility, France).

H₂O₂ experiments

Myoblasts were seeded onto 60 mm collagen-coated dishes, cultured in growth medium containing 10% FCS and treated with several concentrations of H₂O₂ for 24 hrs. For specific experiments, myoblasts were pre-treated (or not) twice with 50 μ M DEAB, 24 hrs and ½ hr before H₂O₂ addition. Dead myoblasts were revealed by staining with ethidium homodimer-1 (2 mM, Sigma-Aldrich) and were analysed by flow cytometry using a FACS Calibur and the CellQuestPro software. Analysis of apoptosis by JC-1, caspase 3/7 and annexin labelling. JC-1 probe (Fluoprobes, Interchim, Montluçon, France) was used for the quantification of depolarized mitochondria. In non-apoptotic cells, JC-1 aggregates in the intact mitochondria resulting in red fluorescence. In apoptotic cells, JC-1 exists in monomeric form and stains cells green. Cells were collected, centrifuged and loaded with 2.5 μ g/ml JC-1 at 37°C for 15 min. Cells were washed, centrifuged and resuspended in 0.5 ml of PBS bovine serum albumin. Cell fluorescence was measured by flow cytometry. Caspases 3/7 activities were assessed by carboxyfluorescein-fluorochrome inhibitor of caspases (FAM-FLICA) reagent (Fluoprobes, Interchim, France). Cells were collected, centrifuged and resuspended in 300 μ l of 1 \times wash buffer and 2 μ l of 150 \times Caspase3/7-FLICA solution were added to the cell suspension. Cells were incubated for 1 hr at 37°C. Cells were then washed, centrifuged and resuspended in 0.5 ml of wash buffer. Samples were kept on ice until FACS analysis. Phosphatidylserine externalization, an early event associated with the onset of apoptosis, was assessed with Annexin V-488 (Fluoprobes, Interchim, France). Briefly, cells were loaded with Annexin V-488 for 15 min. at 37°C. Samples were kept on ice until FACS analysis.

Cell transplantation

All animal surgical procedures were approved by The Institutional Animal Care and Use Committee, Centre anti-cancéreur, Val d'Aurelle-Paul Lamarque, Montpellier, France. *SCID* immunodeficient mice, aged 5 weeks (Charles River, L'Arbresle, France) were anesthetized by intraperitoneal injection of 100 mg/kg ketamin hydrochloride and 10 mg/kg xylasin. Human myoblasts were labelled with intravital fluorescence marker, PKH67 dye (Sigma). As determined by FACS analysis, more than 99% of cells were labelled by PKH67 (data not shown). Immediately after the injection or 2 days after implantation, muscle derived cells were isolated and plated for 24 hrs to recover implanted human cells and host mouse cells. Cells were then analysed by FACS and immunostaining. In a first set of experiments, human myoblasts were pre-treated with DEAB (50 μ M) for 24 hrs and then 2 \times 10⁵ myoblasts were implanted. Control non-treated cells were injected into the right quadriceps and DEAB-treated cells into the left quadriceps of the same mice. Cells were recovered 2 days after implantation. In a second set of experiments, ALDH^{high} (top 5% of the parent population) and ALDH^{low} cells (bottom 5% of the parent population) were selected with FACS ARIA, labelled with PKH67 and then implanted into quadriceps. ALDH^{low} cells were injected in the right quadriceps and ALDH^{high} cells in the left quadriceps of the same mice. Due to the low amount of FACS-sorted myoblasts, we only grafted 1 \times 10⁴ cells. Implanted muscles were harvested immediately after injection to determine accurately the real number of injected cells and then 2 days after implantation. According to the percentage of human cells (quantified by FACS) and the total number of cells (cell counter, Beckman Coulter, Roissy, France), we determined the number of human cells really injected into quadriceps. Statistical analysis was performed with Graph Pad Prism 4.0 Software using t-test.

Results

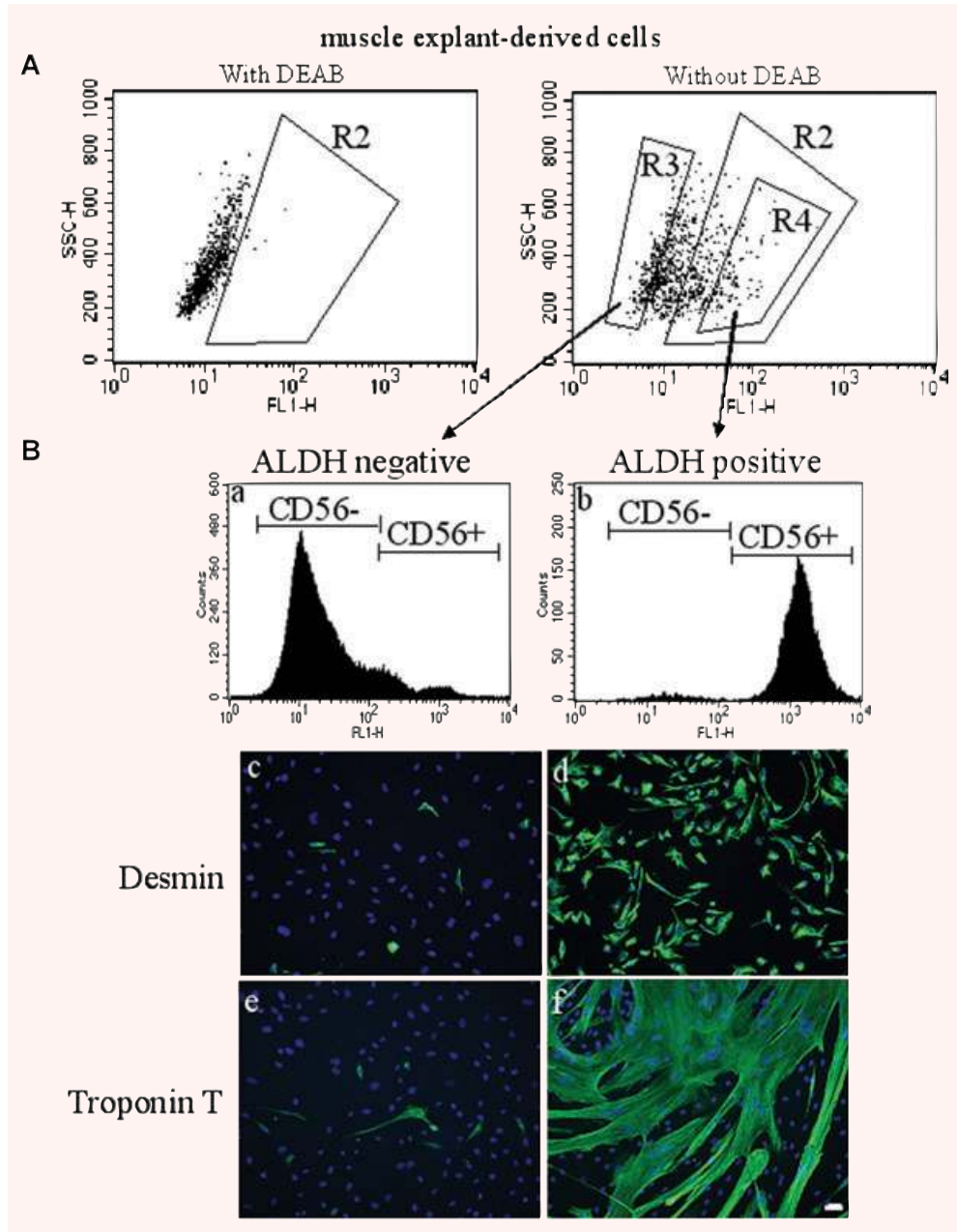
ALDH activity is associated with the myoblast fraction of human skeletal muscle explant-derived cells

To determine whether ALDH activity was detectable in cells associated with skeletal muscle, we first prepared explant-derived cells from cultures of human muscle biopsies. We then incubated these cells with ALDEFLUOR, a fluorescent substrate for ALDH, and determined by FACS the level of enzyme activity. In each experiment, we incubated an aliquot of cells with ALDEFLUOR and DEAB – an inhibitor of ALDH – as a negative control. Analysis of cells derived from 5 different biopsies showed on average 20% ALDEFLUOR⁺ cells (20.1 \pm 4.1 S.E.M.) (Fig. 1A; R2 gate set using DEAB controls). Several and distinct subpopulations of precursor cells are resident in skeletal muscle, nevertheless, myoblasts, the skeletal muscle precursor cells, represent a high percentage of the cells that will migrate from the explants (data not shown; [31, 32]). To determine whether ALDH activity is associated with the myoblast fraction of cells, we plated FACS-sorted ALDH⁺ and ALDH⁻ 'explant-derived' cells. We looked for expression of CD56 and desmin, two markers of muscle precursor cells, by FACS analysis using anti-CD56 antibodies and by immunofluorescence with an anti-desmin antibody. Only ALDH⁺ cells expressed desmin and CD56 in more than 99% of the cells (Fig. 1B). We further confirmed the myoblast identity of those cells by testing their capacity to differentiate into muscle fibres. We grew cells until confluence and then induced muscle differentiation by shifting to differentiating medium (2% FCS). During myogenic differentiation, myoblasts exit the cell cycle and spontaneously differentiate into a major subpopulation of quiescent multinucleated cells (myotubes) that express muscle-specific structural proteins. As expected, only ALDH⁺ cells differentiated into myotubes as shown by troponin T expression (Fig. 1B). To validate these data, we purified myoblasts from explant-derived cells by using an immunomagnetic sorting system coupled with an antibody against CD56 [15, 32].

This technique enabled us to obtain highly purified myoblast cultures with about 99% desmin-positive cells. We then incubated myoblasts (CD56⁺) and non-myoblast cells (CD56⁻) with ALDEFLUOR and analysed ALDH activity by flow cytometry (Fig. 2A). We detected a population of cells with high levels of ALDH staining (not observed when cells were treated with DEAB) only in the CD56⁺ cell fraction. Therefore, these results confirm that only myoblasts possess high ALDH activity. The percentage of ALDH⁺ cells ranged from 38% to 64% of all myoblast cultures (51.3 \pm 2.6 S.E.M.; n = 9) (Fig. 2B), indicating that about 50% of CD56-purified myoblasts exhibited low levels of ALDH activity.

To determine the functional characteristics of myoblasts with high ALDH activity compared to myoblasts with low ALDH activity, we incubated 'CD56-purified' human myoblasts (hm1, hm2 and hm3) with ALDEFLUOR and sorted them by FACS based on

Fig. 1 Characterization of ALDH⁺ cells in muscle explant-derived cells. **(A)** Cytometric analysis of muscle explant-derived cells stained with ALDEFLUOR in the presence (left panel) or not (right panel) of the ALDH inhibitor DEAB. Those cells gated in R2 represent the subpopulation of cells that is positive for ALDH activity. **(B)** Muscle explant-derived cells stained by ALDEFLUOR were sorted into ALDH⁻ cells (R3, bottom 5% of the parent population; a, c, e) and ALDH⁺ (R4, top 5% of the parent population; b, d, f). These two populations of cells were plated and analysed: by cytometric analysis for CD56 expression (a, b); by immunofluorescence for desmin (c, d) and troponin T (e, f) expression (in green). Nuclei were revealed by DAPI (in blue). Bar: 10 μ M.



the levels of ALDH activity. We then seeded ALDH^{high} and ALDH^{low} myoblasts and quantified their ALDH activity by FACS at different time-points after plating. Note that the degree of purification was not absolute because we observed $12\% \pm 2$ of ALDH^{low} myoblasts in the ALDH^{high} population and $15\% \pm 2$ of ALDH^{high} myoblasts in the ALDH^{low} population (Fig. 3A). The percentage of ALDH^{high} myoblasts remained stable in culture. In contrast, the percentage of ALDH^{low} myoblasts, which remained stable during the first 2 days in culture, progressively decrease (Fig. 3A). Such

decrease of ALDH^{low} cell population might be due to a selective advantage of the ALDH^{high} cell population. However, the percentage of dead cells in ALDH^{low} and ALDH^{high} was not statistically different (data not shown) and their proliferative capacities were very similar (Fig. 3B). We then determined in FACS sorted ALDH^{high} and ALDH^{low} myoblasts the pattern of expression of several genes involved in myogenic cell determination such as Pax7, MyoD and Myf5 and confirmed the myogenic identity using anti-desmin antibodies. Western blot analyses showed no differences in Pax7,

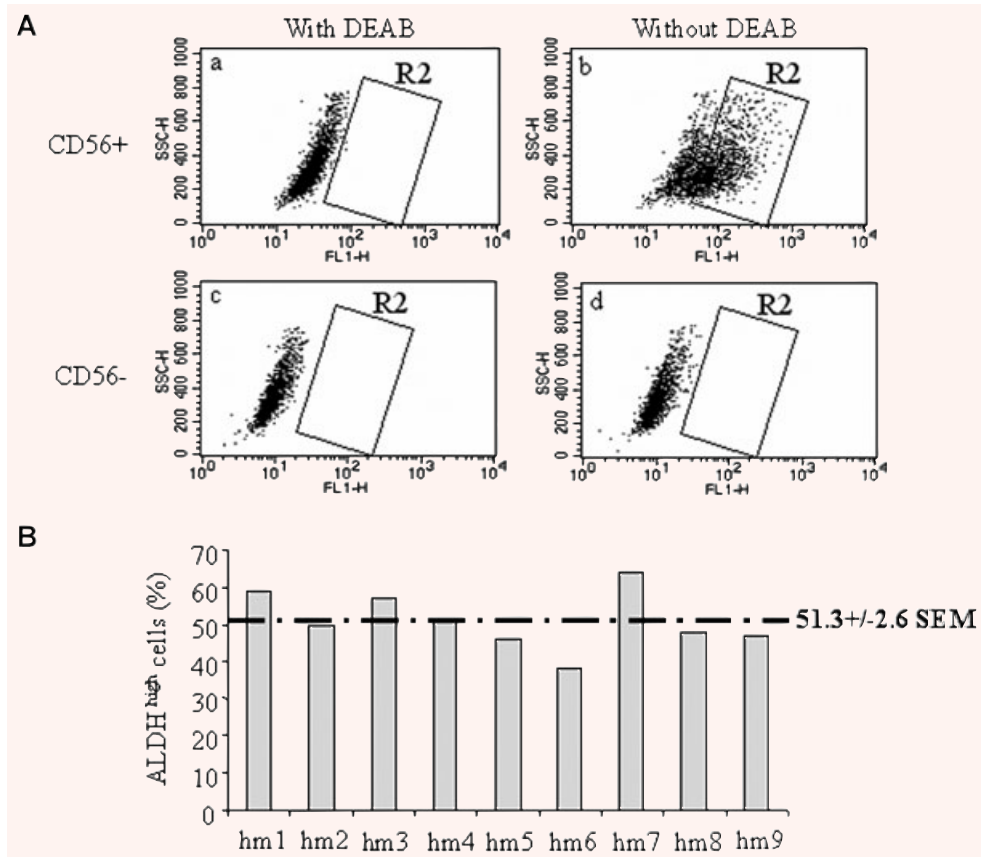


Fig. 2 Human myoblasts are characterized by heterogeneous levels of ALDH activity. Myoblasts from muscle explant-derived cells were purified by using an immuno-magnetic sorting system coupled with an antibody against CD56. **(A)** Cytometric analysis of CD56⁺ (myoblasts; a, b) and CD56⁻ (non-myoblasts; c, d) cells stained with ALDEFUOR in the presence (a, c) or not (b, d) of DEAB. **(B)** Data represent the percentage of cells with high levels of ALDH (ALDH^{high}) in nine different cultures of CD56⁺ human myoblasts (hm1–9). Means 51.3 ± 2.6 S.E.M.; *n* = 9.

MyoD, Myf5 and desmin expression between ALDH^{high} and ALDH^{low} myoblasts (Fig. 3C). Next we wanted to check whether sorted ALDH myoblasts could differentiate normally. We determined by Western blotting the expression of several differentiation markers: slow and fast myosin heavy chain, troponin T and caveolin-3. The level of expression for all these markers was similar in the two populations of cells (Fig. 3D). We also examined myotubes' morphology by immunofluorescence with two differentiation markers, troponinT and myogenin. ALDH^{high} and ALDH^{low} myoblasts fused to form branched myotubes with aligned nuclei (Fig. 3E). Taken together these results indicate that both ALDH^{high} and ALDH^{low} subpopulations of myoblasts differentiated normally and similarly.

Therefore, ALDH activity is a new marker of human myoblasts and can be used to discriminate myoblasts with different levels of ALDH activity.

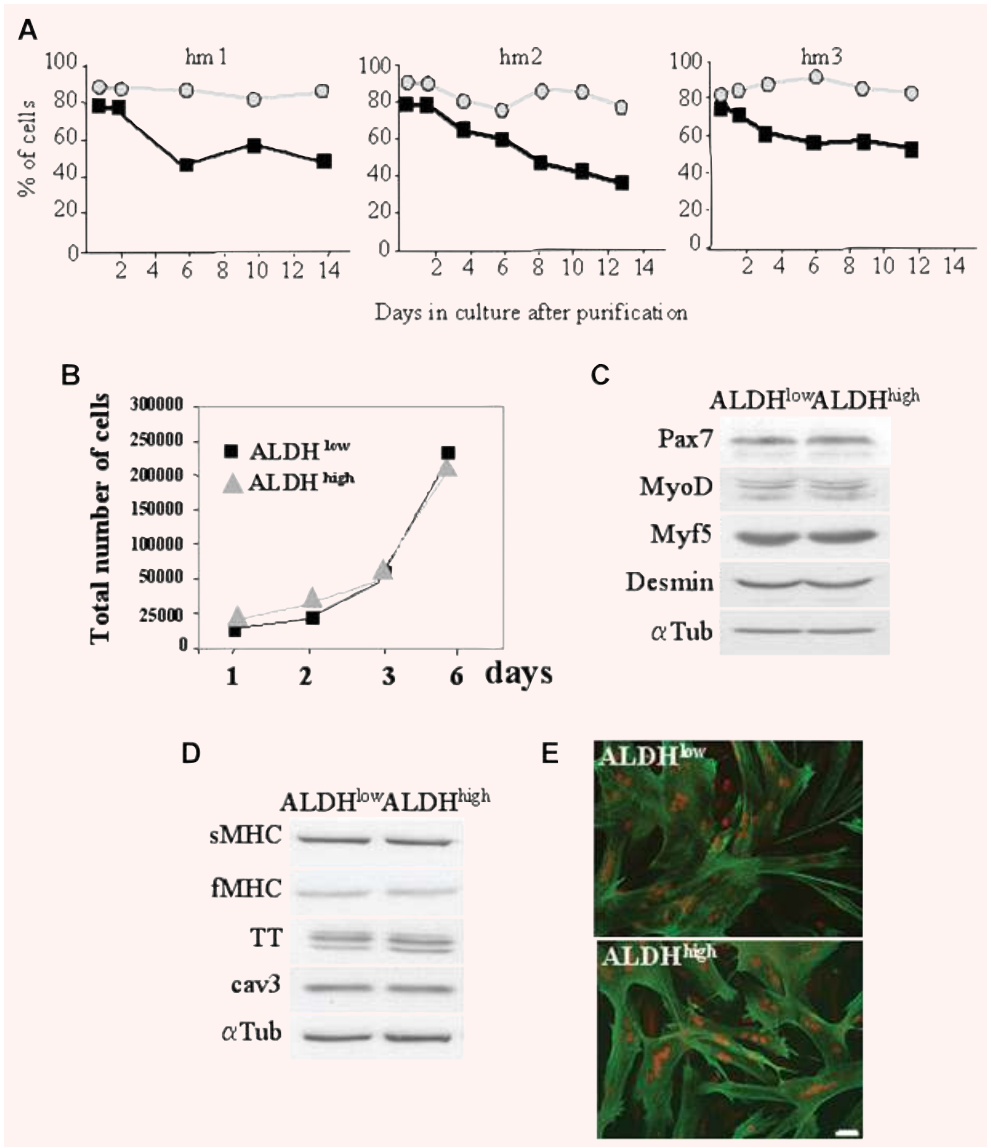
Aldh1a1 expression is associated with ALDH activity in human myoblasts

Two large-scale gene expression analyses of human myoblasts identified Aldh1a1 as the main ALDH protein expressed in muscle cells [33, 34]. Using Western blot analysis, we examined the

expression of Aldh1a1 from CD56⁺ and CD56⁻ 'explant-derived' cells and from FACS sorted ALDH^{high} and ALDH^{low} CD56⁺ myoblasts. Western blot revealed a strong immunoreactive 50 KD band for Aldh1a1 only in CD56⁺ cells (Fig. 4A). Aldh1a1 was expressed mainly in FACS sorted ALDH^{high} myoblasts and not in FACS sorted ALDH^{low} myoblasts (Fig. 4B). Quantitative reverse transcriptase-polymerase chain reaction (RT-PCR) analysis confirmed the strongest level of *Aldh1a1* expression in FACS sorted ALDH^{high} myoblasts (Fig. 4C).

Western blot and quantitative RT-PCR analyses suggested a good correlation between mRNA level of Aldh1a1 and ALDH activity. To determine whether ALDH activity reflects Aldh1a1 expression in human myoblasts, we used lentiviral mediated expression of Aldh1a1 shRNA (Fig. 5). Three constructs targeting different regions of the gene sequence were screened for their efficacy to inhibit Aldh1a1 expression in human myoblasts. Non target-sh lentiviral construct, that does target any human and mouse genes, was used as control. The expression of two specific shRNA, shAldh1a1-98 and Aldh1a1-82, and at a lesser extent shAldh1a1-02, resulted in a marked decrease of Aldh1a1 protein and activity (Fig. 5A and 5B), in comparison to non-infected myoblasts and to the control cells expressing non-target-shRNA. In conclusion, Aldh1a1 contributes to most if not all ALDH activity in human myoblasts.

Fig. 3 Characterization of fractionated ALDH^{high} and ALDH^{low} myoblasts. (A) Fractionated ALDH^{high} (circles; top 5% of the parent population) and ALDH^{low} myoblasts (squares; bottom 5% of the parent population) from clones hm1, hm2, hm3 were analysed for ALDH activity by FACS at different time-points after plating. (B) Sorted ALDH^{high} and ALDH^{low} myoblasts from clone hm1 were analysed for proliferation capacity. Protein extracts from proliferative (C) or differentiated (D) ALDH⁺ and ALDH⁻ myoblasts (clone hm1) were analysed by Western blotting for Pax7, MyoD, Myf5, desmin at the proliferative stage (C), and for fast and slow Myosin Heavy Chain (fMHC, sMHC), troponin T (TT), caveolin 3 (cav3), at the differentiated stage (D). Equal loading control was assessed with α tubulin (α Tub) expression. (E) ALDH⁺ and ALDH⁻ myoblasts (clone hm1) differentiated myotubes were characterized by immunofluorescence using antibodies against troponin T (a microfilament protein; green) and myogenin (a transcription factor; red). Bar : 10 μ M.



High ALDH activity is restricted to human myoblasts

To extend our results to other species, we prepared satellite cells from skeletal muscle of 1-month and 22-month-old mice. After *in vitro* proliferation, we assessed the degree of myoblast purity by immunofluorescence with an anti-desmin antibody: our primary cultures were composed of about 80–85% myoblasts (Table 1). We then analysed mouse myoblasts for ALDH activity. Surprisingly, we were unable to detect significant ALDH activity in those cultures (Fig. 6A, upper panels; Table 1). Similar results were obtained using mouse myoblasts C2 cell line (Table 1).

Because the ALDEFLUOR assay kit has been developed for human cells, we asked whether it was specific for human ALDH. To test this possibility, we prepared mice primary cultures of cornea cells, a tissue rich in ALDH [17]. A significant proportion of cornea cells expressed high levels of ALDH activity (Fig. 6A, lower panels), indicating that the ALDEFLUOR assay could identify both human and mouse ALDH. We then investigated whether myoblasts isolated from adult rat, rabbit and non-human primates presented ALDH activity. Myogenicity of these primary cultures was very high as indicated by the presence of 85% to 95% desmin-positive cells. However, we did not detect ALDH activity in any of these cultures using the ALDEFLUOR assay (Table 1), suggesting that

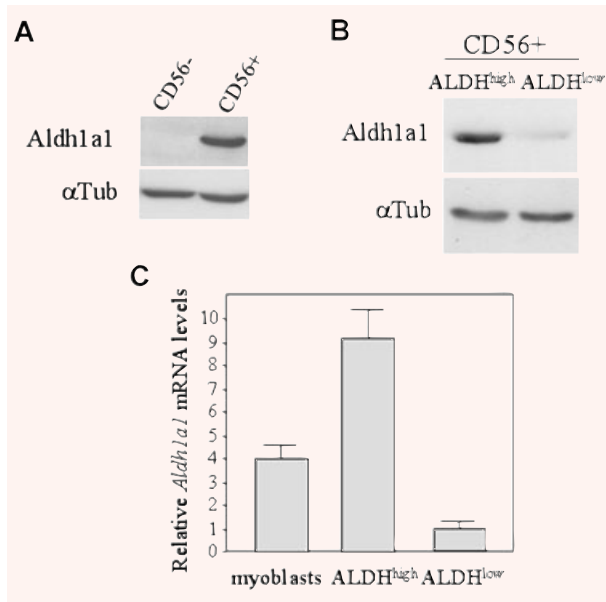


Fig. 4 Aldh1a1 expression is associated with ALDH activity. **(A)** Proteins extracts from CD56⁺ myoblasts and CD56⁻ cells were analysed for Aldh1a1 expression. **(B)** Fractionated ALDH^{high} and ALDH^{low} myoblasts (clone hm1 myoblasts) were analysed for Aldh1a1 expression. Loading control was assessed with α tubulin (α Tub) expression. **(C)** Quantitative reverse transcriptase-polymerase chain reaction analysis (RT-PCR) of relative levels of *Aldh1a1* mRNA in human myoblasts (myoblasts) and in fractionated ALDH^{high} and ALDH^{low} human myoblasts (clone hm1 myoblasts). Expression was normalized against 28s rRNA and the lowest level of *Aldh1a1* expression was set at 1. Means were given \pm S.E.M.; $n = 3$.

ALDH⁺ cells were very rare in adult mouse, rat, rabbit and non-human primates compared to human, below the level of detection by ALDEFLUOR staining.

To isolate myoblasts from mouse, rat, rabbit and non-human primates we followed a protocol of enzymatic digestion with collagenase or pronase (see Materials and Methods), whereas for human myoblasts, due to the low amount of available muscle tissue, we used the 'explant method' and purification with an immunomagnetic sorting system and CD56 antibodies. Such differences in protocols might select specific populations of myoblasts harbouring different levels of ALDH activity. Therefore, we have isolated human myoblasts with pronase digestion following the protocol used for mouse, rat and rabbit muscles. We obtained 85% of desmin-positive cells and found that about 30% to 40% of them were also ALDH⁺ (Table 1). Hence, the method used to isolate myoblasts did not alter the percentage of ALDH⁺ cells. In addition, we showed that Aldh1a1 protein level was very high in mouse cornea cells and in human myoblasts whereas it was below the level of detection by Western blot in mouse, rat, rabbit and non-human primate myoblasts (Fig. 6B). Quantitative RT-PCR analysis confirmed the

lowest level of *Aldh1a1* expression in mouse primary myoblasts, similar to the level observed in human ALDH^{low} myoblasts. As expected, *Aldh1a1* mRNA levels are high in mouse cornea cells and human ALDH^{high} myoblasts (Fig. 6C).

These data highlight fundamental differences in levels of ALDH activity between human and mouse, rat, rabbit and non-human primate myoblasts.

ALDH protects human myoblasts from cytotoxic effects induced by H₂O₂

It has been suggested that Aldh1a1, in addition to its role in aldehyde oxidation, may contribute to the antioxidant capacity of cells [35]. To determine whether inhibition of ALDH activity affected myoblast viability, we pre-treated human myoblasts with DEAB and then exposed them to increasing concentrations of H₂O₂, a pro-apoptotic compound, for 24 hrs (Fig. 7). We quantified the percentage of dead cells by FACS using ethidium homodimer-1 which can only cross the damaged membranes of dead cells. Dead cells could thus be easily distinguished from healthy cells by a bright red fluorescence resulting from staining of nucleic acids by ethidium homodimer-1 [36]. Increasing concentrations of H₂O₂ induced accumulation of dead cells (Fig. 7A). DEAB alone did not affect cell viability. However, concomitant treatment with H₂O₂ and DEAB dramatically enhanced the percentage of dead cells for each concentration of H₂O₂. This synergistic effect occurred also in the presence of a concentration of H₂O₂ (*i.e.* 400 μ M) that on its own did not affect cell viability. We observed this synergistic effect in the three different cultures of human myoblasts we tested (hm1, hm2 and hm3) (Fig. 7A). We then addressed the mechanism of cell death in human myoblasts treated with DEAB. Apoptosis is a term applied to a group of structural and molecular events that separate this type of cell death from necrosis. Depolarized mitochondria, caspases 3/7 activity and phosphatidylserine externalization, which are critical events in the apoptotic process induced by H₂O₂ [37], were assessed by labelling with JC-1, fluorescent caspase 3/7 substrate and Annexin V-488, respectively. A total of 400 μ M H₂O₂ or DEAB alone did not enhance caspase 3/7 activity, the percentage of JC-1 green cells and Annexin V positive cells (Fig. 7B). However, concomitant treatment with H₂O₂ and DEAB dramatically enhanced the percentage of apoptotic cells characterized by caspase 3/7 activity, JC1-green staining and Annexin V positive labelling (Fig. 7B).

We then determined the resistance of ALDH^{high} and ALDH^{low} to H₂O₂ treatment. We treated sorted ALDH^{high} and ALDH^{low} from the three cultures (hm1, hm2, hm3) of human myoblasts with increasing concentrations of H₂O₂ for 24 hrs and determined the percentage of dead cells by FACS analysis after ethidium homodimer-1 staining. ALDH^{high} myoblasts were more resistant to H₂O₂-induced cell death than ALDH^{low} myoblasts (Fig. 7C). These data suggest that ALDH protects human myoblasts against apoptotic effects induced by H₂O₂.

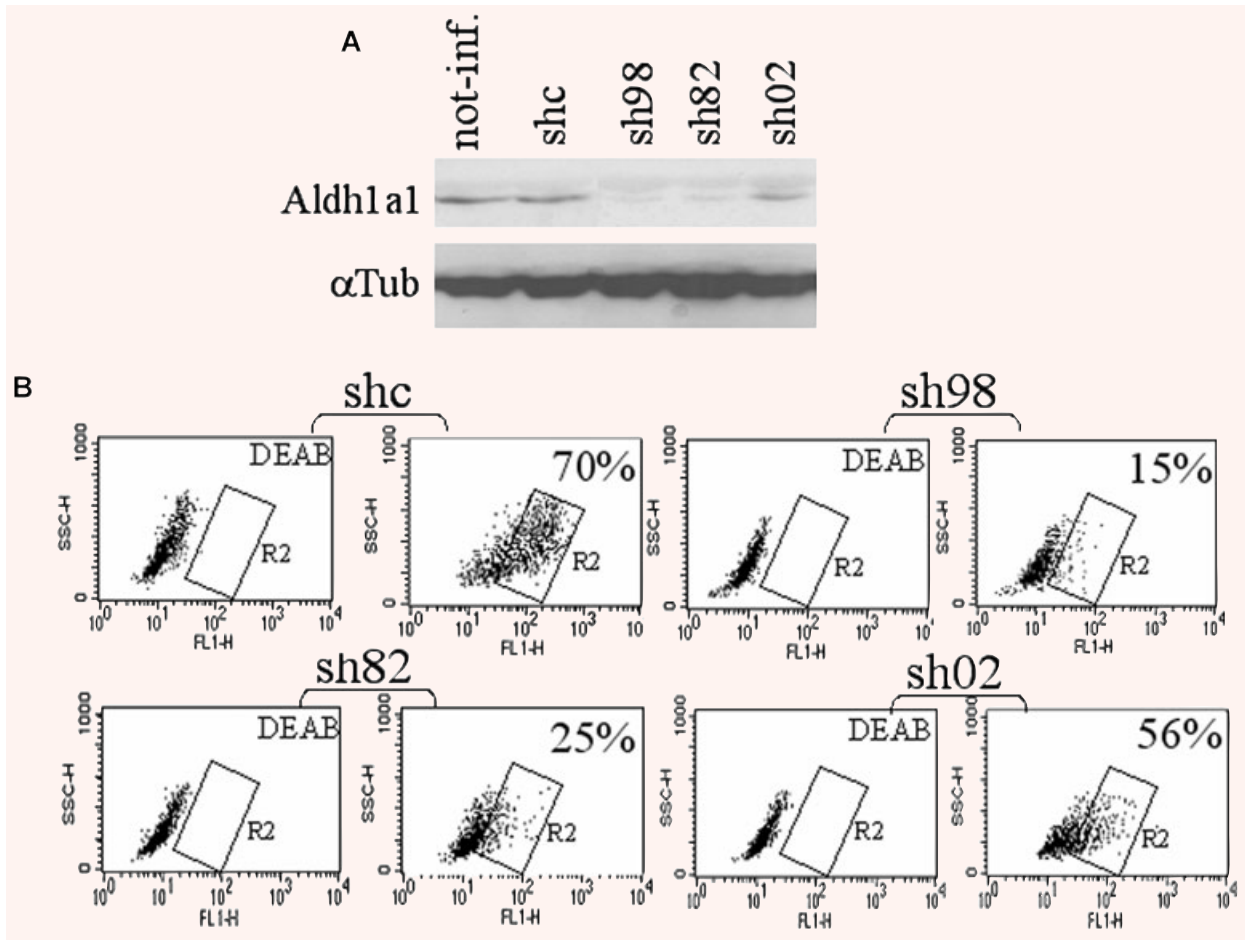


Fig. 5 Aldh1a1 contributes to most if not all ALDH activity in human myoblasts. **(A, B)** Human myoblasts, transduced or not (not-inf.) with lentiviral mediated expression of control shRNA (shc) or Aldh1a1 shRNA (sh98, sh82, sh02) were analysed for Aldh1a1 expression by Western blot **(A)** and ALDH activity in the presence or not of DEAB by FACS **(B)**.

ALDH activity promotes survival of engrafted human myoblasts

We investigated whether we could correlate high ALDH activity to increased cell survival 2 days after implantation into the muscle of adult recipient. In order to track human myoblasts after transplantation, cells were labelled with intravital fluorescence marker, PKH67 dye [38, 39]. In preliminary *in vivo* experiments, we injected labelled myoblasts in quadriceps of *scid* mouse. Two days after implantation, muscle derived cells were isolated and plated for 24 hrs to recover implanted human cells and host mouse cells. Cells were then analysed by FACS and immunostaining. A distinct population of PKH67^{bright} was clearly identified by FACS analysis whereas no fluorescent cells were detected in muscle derived cells of control non-injected *scid* mice (Fig. 8A). Immunostaining for human CD56 revealed that PKH67 labelled cells were also CD56⁺ (Fig. 8B, left; CD56 in red, PKH67 in

Table 1 ALDH activity in myoblast from different species. Recapitulative data from myoblast cultures from different mammalian species. The index of myogenicity was determined as the percentage of desmin positive cells (number of desmin positive cells divided by the total number of DAPI-stained nuclei).

Type of myoblasts	Myogenicity (%)	ALDH activity (%)
Human myoblasts (CD56 purified)	99	58
Human myoblasts (pronase treatment)	85	36
Mouse myoblasts (1 month)	85	0
Mouse myoblasts (22 months)	80	0
Mouse C2 cell line	100	0
Rat myoblasts	85	0
Rabbit myoblasts	90	0

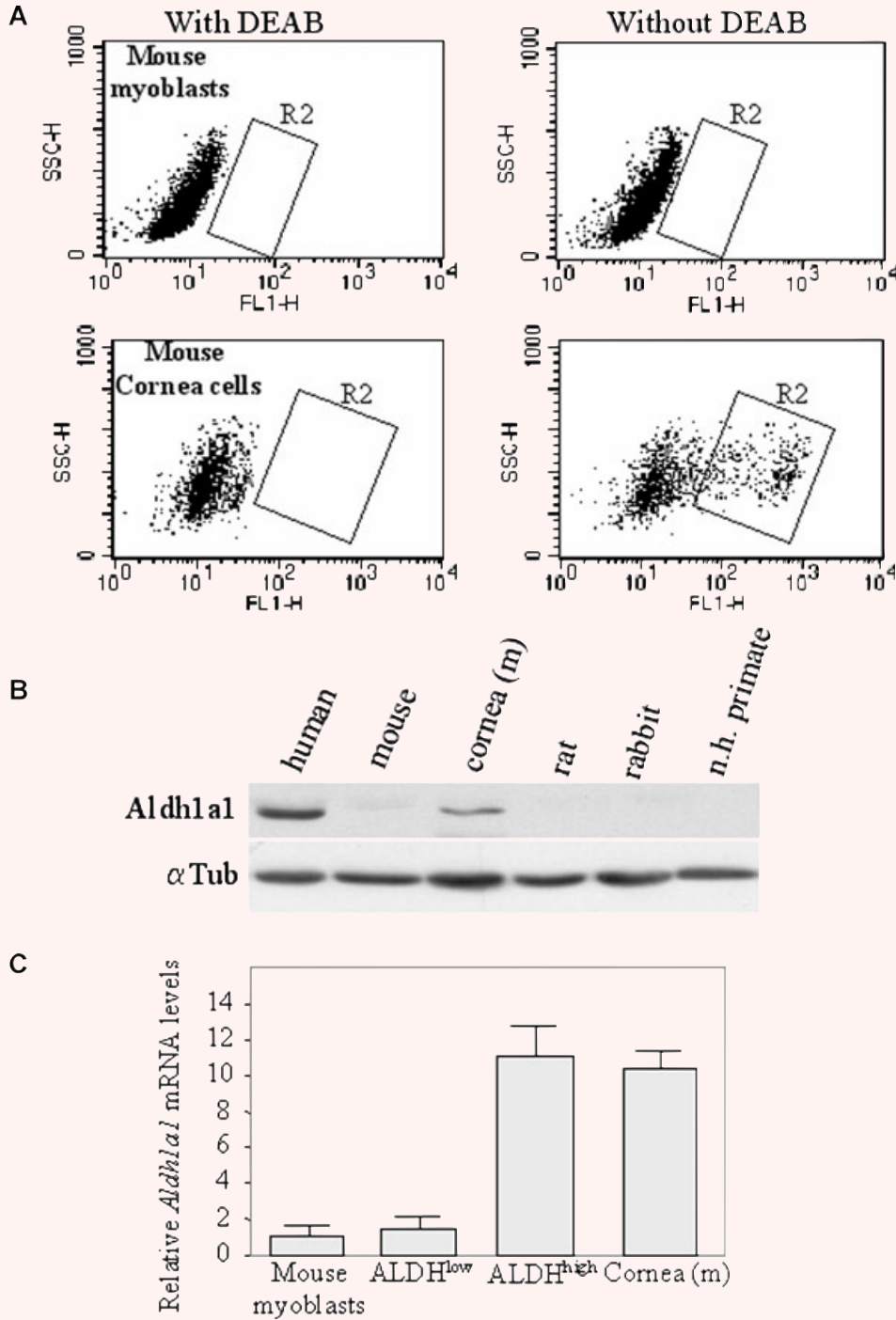
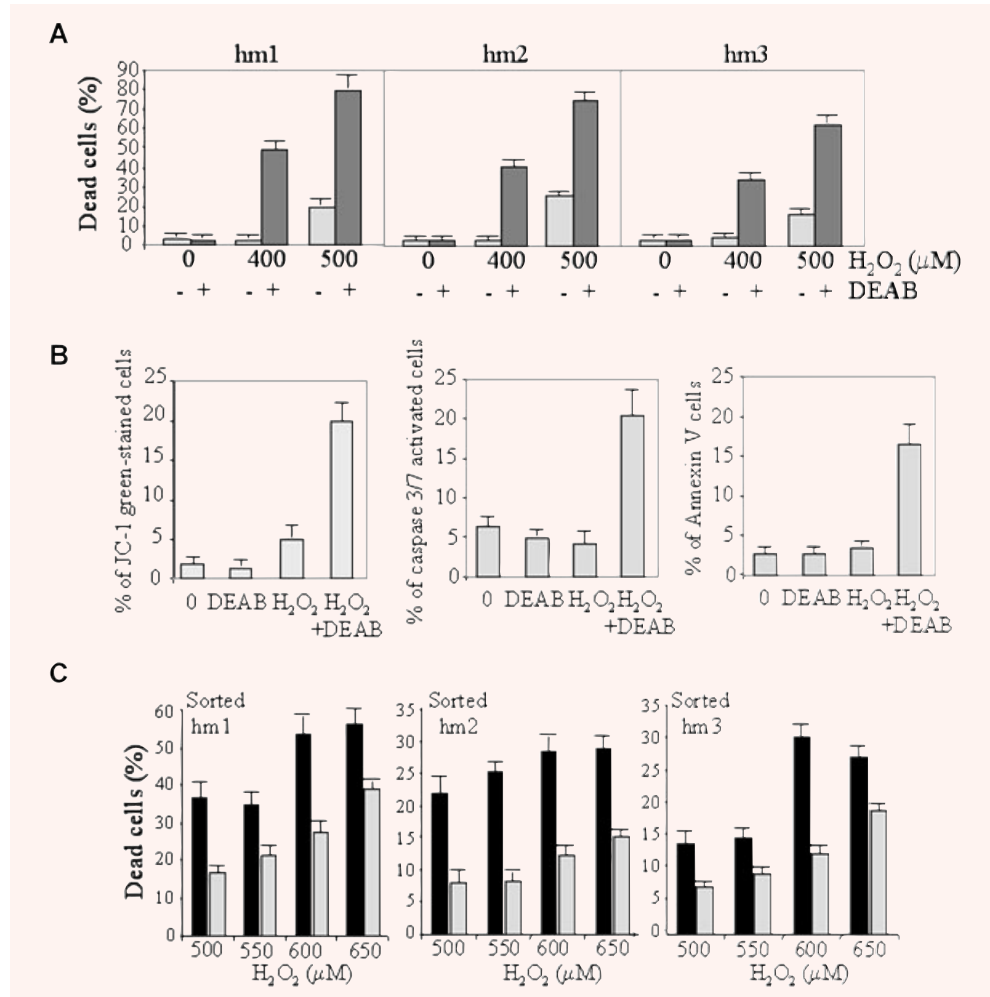


Fig. 6 High ALDH activity and *Aldh1a1* expression are restricted to human myoblasts. **(A)** Primary cultures of mouse myoblasts (upper panels) and cornea cells (lower panels) were stained with ALDEFLUOR in the presence (left panels) or not (right panels) of DEAB and analysed by FACS. **(B)** Protein extracts from human myoblasts (human), mouse myoblasts (mouse), mouse cornea cells (cornea (m)), rat myoblasts (rat), rabbit myoblasts (rabbit) and non-human primate myoblasts (n.h. primate) were analysed for *Aldh1a1* expression. Loading control was assessed with α tubulin (α Tub) expression. **(C)** Quantitative reverse transcriptase-polymerase chain reaction analysis (RT-PCR) of relative levels of *Aldh1a1* mRNA in mouse myoblasts, fractionated ALDH^{high} and ALDH^{low} human myoblasts and in mouse cornea cells. Expression was normalized against *28s* rRNA and the lowest level of *Aldh1a1* expression was set at 1. Means were given \pm S.E.M.; $n = 3$.

Fig. 7 High ALDH activity increases myoblast resistance to H₂O₂-induced cell death. **(A)** Data represent the percentage of dead cells quantified by FACS after ethidium homodimer-1 staining in clones hm1, hm2, hm3 after treatments with H₂O₂ (light grey bars) or H₂O₂ + DEAB (dark grey bars). Means were given ±S.E.M.; n = 3. **(B)** Data represent the percentage of apoptotic cells quantified by FACS after JC-1, caspase 3/7 and Annexin V staining in clones hm1 after treatments with H₂O₂ (400 μM), DEAB (50 μM) or H₂O₂ + DEAB. Means were given ±S.E.M.; n = 3. **(C)** Sorted ALDH^{low} myoblasts (black bars) and ALDH^{high} (light grey bars) were plated and treated with increasing concentrations of H₂O₂ for 24 hrs. The percentages of dead cells were determined by FACS analysis after ethidium homodimer-1 staining. Means were given ±S.E.M.; n = 3.



green). Conversely, mouse cells, identified by the absence of CD56 staining, were not labelled by PKH67. Sections of injected muscle were stained with human specific lamin A/C antibodies. Muscle of injected animals contained mononucleated human lamin A/C⁺ cells (red in Fig. 8B, right). PKH67 labelling was restricted to lamin A/C⁺ cells and did not diffuse to adjacent dystrophin-positive myofibres (purple in Fig. 8B). Taken together these data indicated that PKH67 did not diffuse from human to mouse cells. Therefore, PKH67 is a reliable tracking agent for identifying exogenous human myoblasts in histological sections and by flow cytometry.

We next investigated whether pre-treatment of myoblasts with DEAB could alter their survival in *in vivo* experiments. PKH67 labelled human myoblasts, pre-treated with DEAB, were implanted into muscle of *scid* mouse. Two days after implantation, muscle derived cells were harvested and analysed by FACS. As shown in Fig. 8C, pre-treatment with DEAB reduced by 40% the number of human myoblasts recovered after transplantation. We then determined the resistance to transplantation of ALDH^{high} and ALDH^{low}

myoblasts. We incubated 'CD56-purified' human myoblasts with ALDEFUOR and sorted them by FACS based on the levels of ALDH activity. Sorted ALDH^{high} and ALDH^{low} cells were labelled with PKH67 and implanted into quadriceps muscles of *scid* mouse. Muscles were harvested immediately or 2 days after implantation and the number of human myoblasts was determined by FACS analysis. The average number of ALDH^{high} cells was moderately reduced by about 36% 2 days after implantation. In contrast, we observed a dramatic disappearance of implanted ALDH^{low} cells, because about 75% of those cells were eliminated 2 days after implantation (Fig. 8D).

Discussion

Mouse and human satellite cells have been shown to be functional muscle stem cells, in that they are able to regenerate skeletal muscle and to reconstitute the satellite cell pool [40–42]. More

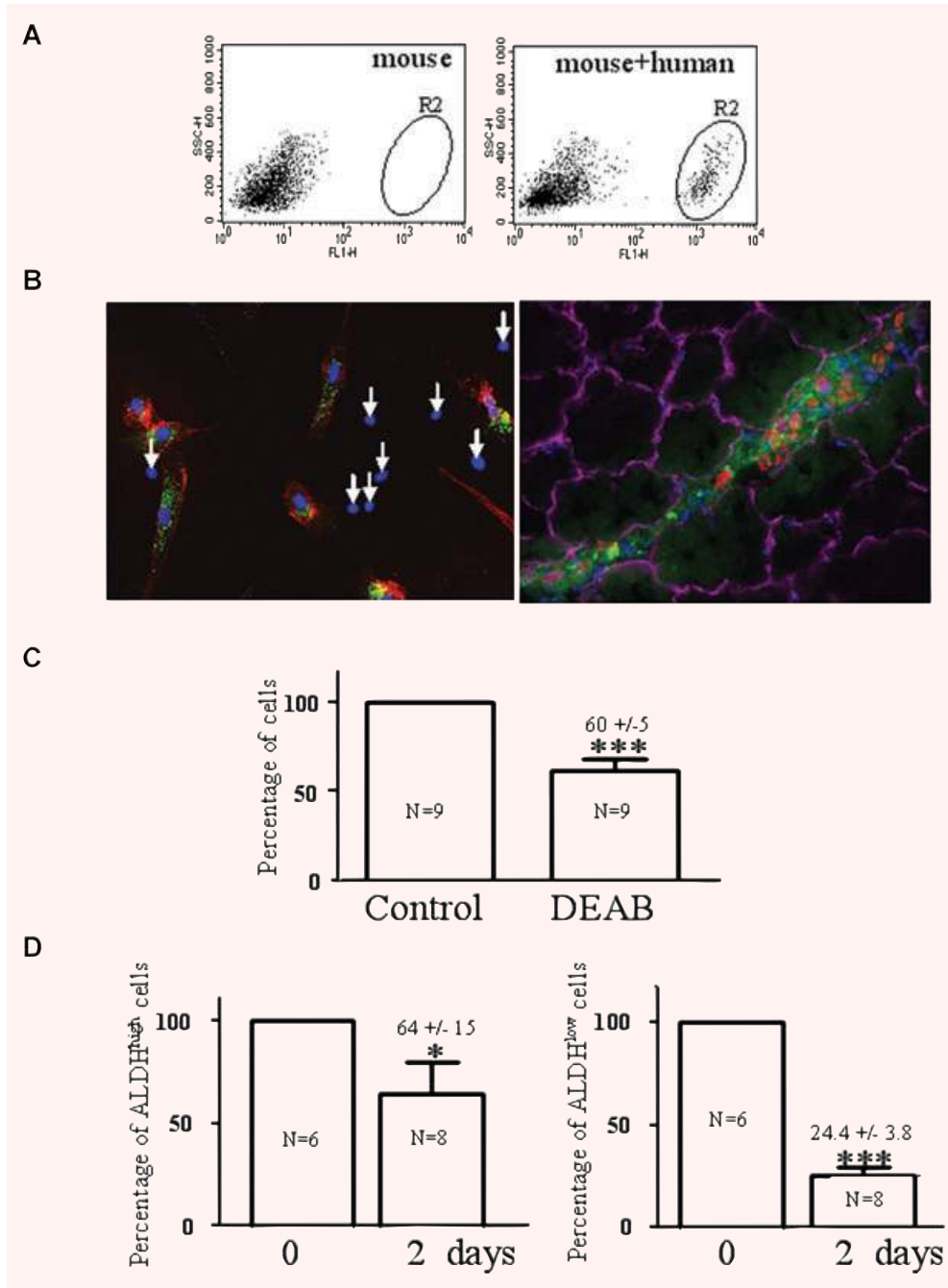


Fig. 8 High ALDH activity is correlated with improved cell survival in grafting experiments. (A, B) PKH67 labelled human myoblasts (green) were implanted into quadriceps of *scid* mouse. Two days after implantation, muscle derived cells were isolated from implanted quadriceps and plated for 24 hrs to recover cells. Non-implanted quadriceps was used as control. Cells were analysed in parallel for PKH67 by FACS (A) non implanted cells, left panel; implanted human myoblasts, right panel. R2 visualized the bright green fluorescence human myoblasts); for PK67 (green) and human CD56 (red) by immunostaining (B, left panel). Arrows: CD56⁻ mouse cells were not labelled by PKH67. Nuclei were revealed by DAPI (in blue). (B, right panel) Section of implanted muscle were stained with human specific lamin A/C antibodies (red), dystrophin antibodies (purple) and nuclei were revealed by DAPI (in blue). (C) Human myoblasts, pre-treated (or not) with DEAB (50 μ M) for 24 hrs, labelled with PKH67, were implanted into quadriceps muscle of *scid* mouse (2×10^5 cells per quadriceps). Two days after implantation, muscle derived cells were harvested and

analysed by FACS. According to the percentage of human cells (quantified by FACS) and the total number of cells, we determined the number of human cells really present into host quadriceps muscles. 100% was arbitrary taken for control non-treated myoblasts. *** $P \leq 0.001$; mean values \pm S.E.M. $N = 9$. (D) Sorted ALDH^{high} (left panel) and ALDH^{low} (right panel) human myoblasts were labelled with PKH67 and implanted into quadriceps muscles of *scid* mouse (1×10^4 cells per quadriceps). Muscles were harvested immediately (0) or 2 days (2) after implantation and the number of human myoblasts was determined by FACS analysis. 100% was arbitrary taken for ALDH^{high} (left panel) and ALDH^{low} (right panel) cells immediately after injection. * $P \leq 0.05$ and *** $P \leq 0.001$; mean values \pm S.E.M. $N = 6$ (point 0 days), $N = 8$ (point 2 days).

recently, several groups have shown that increased antioxidant capacity may represent an additional functional characteristic of stem cells [43, 44]. Expanding on this work, Urish *et al.* demonstrated that muscle-derived stem cells in mice were characterized by high antioxidant capacity that enhanced its regenerative capacity [45]. In this study, we identified Aldehydes dehydrogenases, a family of enzymes that efficiently detoxify aldehydic products generated by reactive oxygen species, as a marker of human myoblasts. We demonstrate that 'CD56-purified' human myoblasts contain a fraction of cells with different levels of ALDH activity. By inactivating Aldh1a1 in human myoblasts with lentiviral mediated expression of Aldh1a1 shRNA, we demonstrated that Aldh1a1 contributes to most if not all ALDH activity in human myoblasts. Therefore, these data clearly indicate that others ALDH isoforms do not compensate functionally for Aldh1a1. Consistent with these observations, we did not detect Aldh1a2 and Aldh3a1 expression in human myoblasts (by Western blot and QPCR, respectively; our unpublished observations). Using different approaches, from pharmacological inhibition of ALDH by DEAB to cell fractionation by FACS using the ALDEFUOR assay, we correlate high ALDH activity to improved cell viability.

Our results established that human myoblasts exhibit ALDH activity and Aldh1a1 expression while ALDH activity and Aldh1a1 expression were below detection by ALDEFUOR and immunostaining in mouse, rat, rabbit and non-human primate myoblasts. Similarly, in contrast to ALDH labelling in human haematopoietic tissues, detection of ALDH activity in primitive murine haematopoietic cells is still controversial [46, 47]. Analysis performed in Aldh1a1-deficient mice revealed that Aldh1a1 is dispensable for stem cell function and, in contrast to our results in human, did not contribute to ALDH activity in mouse [47]. It already has been shown that there are species-specific differences in the expression of growth factors and cell surface markers that are crucial for satellite cell function. For example, mouse myoblasts cease to proliferate in culture unless they are exposed to FGF [48], whereas human myoblasts can undergo many divisions in culture. In contrast to mouse, CD34 cells appeared at very low frequency in human myoblasts [15]. Furthermore, antibodies against CD34 cannot identify satellite cells in section of human muscle [49]. These previous results, together with our findings indicate that human myoblasts have acquired additional signalling pathways suggesting that the optimal conditions for muscle regeneration are different in each species.

A major obstacle in myoblast transplantation therapy is the poor rate of cell survival after implantation. A large percentage of myoblasts die within 48 hrs, which correlates with an acute inflammatory response at the site of injection [7]. Recent data suggested that oxidative stress which is presumably derived from damage induced by intramuscular implantation of myoblasts, may cause rapid cell death: antioxidant pre-treatment of myoblasts with CuZn-SOD improves the graft survival [50]. Conversely, inhibition of antioxidant capacity by decreasing glutathione activity reduces the regeneration capacity of muscle-derived stem cells [45]. We postulated that one of the mechanisms behind the higher viability of ALDH^{high} myoblasts

after transplantation may involve a resistance to oxidative stress. We showed that ALDH activity and Aldh1a1 expression were associated to resistance to H₂O₂ treatment, a well-established model to study muscle apoptosis associated with oxidative stress [51]. Concomitant treatment with H₂O₂ and DEAB, an inhibitor of class I ALDH, caused a synergic loss of cell viability. Because ALDH activity is mainly dependent on Aldh1a1 expression in human myoblasts, we tested whether direct inactivation of Aldh1a1 altered cell viability. We first inactivated Aldh1a1 in those cells using lentiviral mediated expression of Aldh1a1 shRNA. However, we cannot analyse our results because control cells expressing non-target-shRNA were abnormally resistant to apoptosis (data not shown). We then determined the resistance of ALDH^{high} and ALDH^{low} myoblasts to H₂O₂ treatment and established that ALDH^{high} myoblasts were more resistant to H₂O₂-induced cell death than ALDH^{low} myoblasts. These data suggest that ALDH activity and Aldh1a1 protect human myoblasts against cytotoxic damages.

Several groups have begun recently to address the question of muscle cell heterogeneity in mice, linking satellite cells' phenotype to function [14, 42, 52]. Based on CD56 and desmin expression, human satellite cells and their progeny (myoblasts) were thought to be homogeneous [15]. However, increasing evidence indicates that human satellite cells are heterogeneous, based on different gene expression associated with different fates [53, 54]. For example, subpopulations of human myoblasts were characterized by their specific proliferation rate, clonogenic and differentiation capacities [53]. At least two subpopulations of human myoblasts have been reported, based on Pax7 expression [54]. Similarly, we found that ALDH⁺ cells in muscle explant-derived cells are myoblasts but not all human myoblasts are ALDH⁺. However, we do not know whether ALDH is present in non-activated satellite cells because we did not manage to obtain an unambiguous endogenous Aldh1a1 signal by immunocytochemistry (unpublished observations). We observed that myoblasts with low ALDH activity generate rapidly in culture myoblasts with high ALDH activity. We checked for cell viability and found that ALDH^{low} did not die preferentially. As shown in Fig. 3, ALDH^{low} and ALDH^{high} proliferate with a similar kinetic. Thus, differences in viability and proliferation cannot explain why the proportion of ALDH^{low} cells decreases. Our results suggest a dynamic equilibrium between these two subpopulations of cells. The molecular mechanisms and the biological significance of such phenomenon remain to be determined. However, we already know that this heterogeneity of expression is associated with a specific function because ALDH^{high} cells are more resistant than ALDH^{low} cells *in vitro*, to cell death initiated by H₂O₂ and *in vivo* following cell transplantation.

Stem cell heterogeneity has been proposed also for cancer cells: only a limited number of cells harbouring specific stem cell antigens can initiate tumours when transplanted into immunodeficient mice [55]. Recently, it has been shown that cells with ALDH activity isolated from normal human breast have characteristics of mammary stem cells. Moreover, ALDH⁺ cells isolated from

human breast tumours include cancer stem cells [23]. Therefore, ALDH activity characterizes a subpopulation of normal and malignant mammary stem cells, supporting the concept of cancer stem cells and cellular heterogeneity.

In conclusion, our study reveals the existence of a subpopulation of human myoblasts characterized by high ALDH activity which appears to confer a survival advantage in cell grafting experiments. Because ALDH activity is observed in haematopoietic, neural, mammary and skeletal muscle stem cells, it could become a useful and non-toxic marker for the detection and isolation of a subpopulation of stem cells with interesting biological properties.

Acknowledgements

This work was funded by the Association Française contre les Myopathies (AFM: G12818A), the Centre National de la Recherche Scientifique (CNRS) and the Institut National de la Santé et de la Recherche Médicale (INSERM). E.J. is recipient of a Ph.D. studentship of Région Languedoc Roussillon and INSERM (number 07-004549). C.N. is supported by a post-doctoral fellowship from the AFM. We thank the Banque de Tissus pour la Recherche of the Association Française contre les Myopathies (AFM). We are grateful to the patients from the 'Association FSHD Europe' who continuously supported this study.

References

- Gnocchi VF, White RB, Ono Y, et al.** Further characterisation of the molecular signature of quiescent and activated mouse muscle satellite cells. *PLoS ONE*. 2009; 4: e5205.
- Partridge TA, Morgan JE, Coulton GR, et al.** Conversion of mdx myofibres from dystrophin-negative to -positive by injection of normal myoblasts. *Nature*. 1989; 337: 176–9.
- Gussoni E, Blau HM, Kunkel LM.** The fate of individual myoblasts after transplantation into muscles of DMD patients. *Nat Med*. 1997; 3: 970–7.
- Peault B, Rudnicki M, Torrente Y, et al.** Stem and progenitor cells in skeletal muscle development, maintenance, and therapy. *Mol Ther*. 2007; 15: 867–77.
- Mendell JR, Kissel JT, Amato AA, et al.** Myoblast transfer in the treatment of Duchenne's muscular dystrophy. *N Engl J Med*. 1995; 333: 832–8.
- Tremblay JP, Malouin F, Roy R, et al.** Results of a triple blind clinical study of myoblast transplantations without immunosuppressive treatment in young boys with Duchenne muscular dystrophy. *Cell Transplant*. 1993; 2: 99–112.
- Beauchamp JR, Morgan JE, Pagel CN, et al.** Dynamics of myoblast transplantation reveal a discrete minority of precursors with stem cell-like properties as the myogenic source. *J Cell Biol*. 1999; 144: 1113–22.
- Kinoshita I, Vilquin JT, Guerette B, et al.** Very efficient myoblast allotransplantation in mice under FK506 immunosuppression. *Muscle Nerve*. 1994; 17: 1407–15.
- Pavlath GK, Rando TA, Blau HM.** Transient immunosuppressive treatment leads to long-term retention of allogeneic myoblasts in hybrid myofibers. *J Cell Biol*. 1994; 127: 1923–32.
- Bouchentouf M, Benabdallah BF, Tremblay JP.** Myoblast survival enhancement and transplantation success improvement by heat-shock treatment in mdx mice. *Transplantation*. 2004; 77: 1349–56.
- Kinoshita I, Vilquin JT, Tremblay JP.** Pretreatment of myoblast cultures with basic fibroblast growth factor increases the efficacy of their transplantation in mdx mice. *Muscle Nerve*. 1995; 18: 834–41.
- Benabdallah BF, Bouchentouf M, Tremblay JP.** Improved success of myoblast transplantation in mdx mice by blocking the myostatin signal. *Transplantation*. 2005; 79: 1696–702.
- Bouchentouf M, Benabdallah BF, Bigey P, et al.** Vascular endothelial growth factor reduced hypoxia-induced death of human myoblasts and improved their engraftment in mouse muscles. *Gene Ther*. 2008; 15: 404–14.
- Cerletti M, Jurga S, Witczak CA, et al.** Highly efficient, functional engraftment of skeletal muscle stem cells in dystrophic muscles. *Cell*. 2008; 134: 37–47.
- Sinanan AC, Hunt NP, Lewis MP.** Human adult craniofacial muscle-derived cells: neural-cell adhesion-molecule (NCAM; CD56)-expressing cells appear to contain multipotential stem cells. *Biotechnol Appl Biochem*. 2004; 40: 25–34.
- Lindstrom M, Thornell LE.** New multiple labelling method for improved satellite cell identification in human muscle: application to a cohort of power-lifters and sedentary men. *Histochem Cell Biol*. 2009; 132: 141–57.
- Vasiliou V, Pappa A, Estey T.** Role of human aldehyde dehydrogenases in endobiotic and xenobiotic metabolism. *Drug Metab Rev*. 2004; 36: 279–99.
- Lassen N, Pappa A, Black WJ, et al.** Antioxidant function of corneal ALDH3A1 in cultured stromal fibroblasts. *Free Radic Biol Med*. 2006; 41: 1459–69.
- Soprano DR, Teets BW, Soprano KJ.** Role of retinoic acid in the differentiation of embryonal carcinoma and embryonic stem cells. *Vitam Horm*. 2007; 75: 69–95.
- Storms RW, Trujillo AP, Springer JB, et al.** Isolation of primitive human hematopoietic progenitors on the basis of aldehyde dehydrogenase activity. *Proc Natl Acad Sci USA*. 1999; 96: 9118–23.
- Hess DA, Wirthlin L, Craft TP, et al.** Selection based on CD133 and high aldehyde dehydrogenase activity isolates long-term reconstituting human hematopoietic stem cells. *Blood*. 2006; 107: 2162–9.
- Corti S, Locatelli F, Papadimitriou D, et al.** Identification of a primitive brain-derived neural stem cell population based on aldehyde dehydrogenase activity. *Stem Cells*. 2006; 24: 975–85.
- Ginestier C, Hur MH, Charafe-Jauffret E, et al.** ALDH1 is a marker of normal and malignant human mammary stem cells and a predictor of poor clinical outcome. *Cell Stem Cell*. 2007; 1: 555–67.
- Croker AK, Goodale D, Chu J, et al.** High aldehyde dehydrogenase and expression of cancer stem cell markers selects for breast cancer cells with enhanced malignant and metastatic ability. *J Cell Mol Med*. 2008.
- Descamps S, Arzouk H, Bacou F, et al.** Inhibition of myoblast differentiation by Srp1 and Srp2. *Cell Tissue Res*. 2008; 332: 299–306.
- Levin JM, El Andaloussi RA, Dainat J, et al.** SFRP2 expression in rabbit myogenic progenitor cells and in adult skeletal muscles. *J Muscle Res Cell Motil*. 2001; 22: 361–9.
- Marelli D, Desrosiers C, el-Alfy M, et al.** Cell transplantation for myocardial repair:

- an experimental approach. *Cell Transplant.* 1992; 1: 383–90.
28. **Chiu RC, Zibaitis A, Kao RL.** Cellular cardiomyoplasty: myocardial regeneration with satellite cell implantation. *Ann Thorac Surg.* 1995; 60: 12–8.
 29. **Li W, Sabater AL, Chen YT, et al.** A novel method of isolation, preservation, and expansion of human corneal endothelial cells. *Invest Ophthalmol Vis Sci.* 2007; 48: 614–20.
 30. **Royuela M, Chazalette D, Rivier F, et al.** Dystrophin and dystrophin-associated protein in muscles and nerves from monkey. *Eur J Histochem.* 2003; 47: 29–38.
 31. **Barro M, Carnac G, Flavier S, et al.** Myoblasts from affected and non affected FSHD muscles exhibit morphological differentiation defects. *J Cell Mol Med.* 2010; 14: 275–89.
 32. **Kitzmann M, Bonniou A, Duret C, et al.** Inhibition of Notch signaling induces myotube hypertrophy by recruiting a subpopulation of reserve cells. *J Cell Physiol.* 2006; 208: 538–48.
 33. **Sterrenburg E, Turk R, t Hoen PA, et al.** Large-scale gene expression analysis of human skeletal myoblast differentiation. *Neuromuscul Disord.* 2004; 14: 507–18.
 34. **Gonnet F, Bouazza B, Millot GA, et al.** Proteome analysis of differentiating human myoblasts by dialysis-assisted two-dimensional gel electrophoresis (DAGE). *Proteomics.* 2008; 8: 264–78.
 35. **Vasiliou V, Nebert DW.** Analysis and update of the human aldehyde dehydrogenase (ALDH) gene family. *Hum Genomics.* 2005; 2: 138–43.
 36. **Papadopoulos NG, Dedoussis GV, Spanakos G, et al.** An improved fluorescence assay for the determination of lymphocyte-mediated cytotoxicity using flow cytometry. *J Immunol Methods.* 1994; 177: 101–11.
 37. **Shan P, Pu J, Yuan A, et al.** RXR agonists inhibit oxidative stress-induced apoptosis in H9c2 rat ventricular cells. *Biochem Biophys Res Commun.* 2008; 375: 628–33.
 38. **Gulbins H, Schrepfer S, Uhlig A, et al.** Myoblasts survive intracardiac transfer and divide further after transplantation. *Heart Surg Forum.* 2002; 5: 340–4.
 39. **Torrente Y, Belicchi M, Sampaolesi M, et al.** Human circulating AC133(+) stem cells restore dystrophin expression and ameliorate function in dystrophic skeletal muscle. *J Clin Invest.* 2004; 114: 182–95.
 40. **Zammit PS.** All muscle satellite cells are equal, but are some more equal than others? *J Cell Sci.* 2008; 121: 2975–82.
 41. **Ehrhardt J, Brimah K, Adkin C, et al.** Human muscle precursor cells give rise to functional satellite cells *in vivo*. *Neuromuscul Disord.* 2007; 17: 631–8.
 42. **Collins CA, Olsen I, Zammit PS, et al.** Stem cell function, self-renewal, and behavioral heterogeneity of cells from the adult muscle satellite cell niche. *Cell.* 2005; 122: 289–301.
 43. **Dernbach E, Urbich C, Brandes RP, et al.** Antioxidative stress-associated genes in circulating progenitor cells: evidence for enhanced resistance against oxidative stress. *Blood.* 2004; 104: 3591–7.
 44. **He T, Peterson TE, Holmuhamedov EL, et al.** Human endothelial progenitor cells tolerate oxidative stress due to intrinsically high expression of manganese superoxide dismutase. *Arterioscler Thromb Vasc Biol.* 2004; 24: 2021–7.
 45. **Urish KL, Vella JB, Okada M, et al.** Antioxidant levels represent a major determinant in the regenerative capacity of muscle stem cells. *Mol Biol Cell.* 2009; 20: 509–20.
 46. **Pearce DJ, Bonnet D.** The combined use of Hoechst efflux ability and aldehyde dehydrogenase activity to identify murine and human hematopoietic stem cells. *Exp Hematol.* 2007; 35: 1437–46.
 47. **Levi BP, Yilmaz OH, Duester G, et al.** Aldehyde dehydrogenase 1a1 is dispensable for stem cell function in the mouse hematopoietic and nervous systems. *Blood.* 2009; 113: 1670–80.
 48. **Linkhart TA, Clegg CH, Hauschka SD.** Control of mouse myoblast commitment to terminal differentiation by mitogens. *J Supramol Struct.* 1980; 14: 483–98.
 49. **Dreyer HC, Blanco CE, Sattler FR, et al.** Satellite cell numbers in young and older men 24 hours after eccentric exercise. *Muscle Nerve.* 2006; 33: 242–53.
 50. **Suzuki K, Murtuza B, Beauchamp JR, et al.** Dynamics and mediators of acute graft attrition after myoblast transplantation to the heart. *FASEB J.* 2004; 18: 1153–5.
 51. **Stangel M, Zettl UK, Mix E, et al.** H2O2 and nitric oxide-mediated oxidative stress induce apoptosis in rat skeletal muscle myoblasts. *J Neuropathol Exp Neurol.* 1996; 55: 36–43.
 52. **Kuang S, Kuroda K, Le Grand F, et al.** Asymmetric self-renewal and commitment of satellite stem cells in muscle. *Cell.* 2007; 129: 999–1010.
 53. **Baroffio A, Bochaton-Piallat M, Gabbiani G, et al.** Heterogeneity in the progeny of single human muscle satellite cells. *Differentiation.* 1995; 59: 259–68.
 54. **Reimann J, Brimah K, Schroder R, et al.** Pax7 distribution in human skeletal muscle biopsies and myogenic tissue cultures. *Cell Tissue Res.* 2004; 315: 233–42.
 55. **Gil J, Stembalska A, Pesz KA, et al.** Cancer stem cells: the theory and perspectives in cancer therapy. *J Appl Genet.* 2008; 49: 193–9.